Bioactive Ceramic Surface Modification of β-Type Ti-Nb-Ta-Zr System Alloy by Alkali Solution Treatment

著者	Akahori Toshikazu, Niinomi Mitsuo, Nakai Masaaki, Fukuda Hidetsugu, Fukui Hisao, Ogawa Michiharu
journal or publication title	Materials Transactions
volume	48
number	3
page range	293-300
year	2007
URL	http://hdl.handle.net/10097/52181

Materials Transactions, Vol. 48, No. 3 (2007) pp. 293 to 300
Special Issue on Smart and Harmonic Biomaterials

Bioactive Ceramic Surface Modification of β-Type Ti-Nb-Ta-Zr System Alloy by Alkali Solution Treatment

Toshikazu Akahori[1], Mitsuo Niinomi[1], Masaaki Nakai[1], Hidetsugu Fukuda*, Hisao Fukui[2] and Michiharu Ogawa[3]

[1]*Department of Biomaterials Science, Institute for Materials Research, Tohoku University, Sendai 980-8577, Japan*
[2]*School of Dentistry, Aichi-Gakuin University, Nagoya 464-8650, Japan*
[3]*R & D Laboratory, Daido Steel Co., Ltd., Nagoya 457-8584, Japan*

Biomedical β-type titanium alloys have been developed or are under development all over the world. In particular, researchers in Japan have been developed Ti-29Nb-13Ta-4.6Zr alloy (TNTZ)—β-type titanium alloy—for biomedical applications. Bioactive ceramic surface modification is effective for further improvement in the biocompatibility of TNTZ. Calcium phosphate ceramics such as hydroxyapatite ($Ca_{10}(PO_4)_6OH_2$; HAP), β-calcium pyrophosphate (β-$Ca_2P_2O_7$; CPP), and β-tricalcium phosphate (β-$Ca_3(PO_4)_2$; β-TCP) exhibit bioactivity. In this study, the formability and morphology of HAP on the surface of TNTZ, covered with sodium titanate film by alkali solution treatment were investigated before and after immersion in a simulated body fluid (SBF).

A reticulate structure with a considerable number of large cracks and mainly composed of sodium titanate and niobate films having a thickness of 400 nm to 800 nm is formed on the specimen surface of TNTZ after immersing in 3, 5, and 10 kmol·m^{-3} NaOH solutions for 86.4 and 172.8 ks. As the concentration of the alkali solution and the immersion time are increased, the formability of HAP improves because of the presence of a large amount of oxygen and the sodium in sodium titanate and niobate film. HAP is completely formed on the entire specimen surface of TNTZ immersed in the SBF for 1209.6 ks after immersing in 5 and 10 kmol·m^{-3} NaOH solutions for 172.8 ks. Alkali treatment at 333 K in 5 kmol·m^{-3} NaOH solutions for 172.8 ks is proposed to be an excellent condition to rapidly form HAP and fully cover the specimen surface of TNTZ with it. The bonding strength between TNTZ (alkali treatment at 333 K in 5 kmol·m^{-3} NaOH solutions for 172.8 ks) and HAP is around 2 MPa, which was half or less than half the value required for biomedical applications. The inclusion of a baking treatment after the alkali treatment in order to improve the bonding strength degraded the HAP formability. Furthermore, the formability decreases with an increase in the baking temperature. [doi:10.2320/matertrans.48.293]

(Received August 29, 2006; Accepted November 22, 2006; Published February 25, 2007)

Keywords: *titanium-29 mass%niobium-13 mass%tantalum-4.6 mass%zirconium, hydroxyapatite, sodium titanate, sodium niobate, simulated body fluid, tensile bonding strength*

1. Introduction

Metallic biomaterials are popularly used as orthopedic implants even in highly loaded parts such as the stems of artificial hip joints. Hence, they are required to possess certain special mechanical, physical, chemical, or biological properties such as high strength, corrosion resistance, bioactivity, or low Young's modulus close to that of a human bone. For many years, the most commonly used metallic materials in medical applications were 316 L stainless steel, Co-Cr-based alloys, commercially pure (CP) titanium, and Ti-6Al-4V extra-low interstitial (ELI) alloy.

Recently, certain new titanium (Ti) alloys composed of β-stabilizers such as niobium (Nb) and tantalum (Ta), a neutral alloying element such as zirconium (Zr), and interstitial oxygen (O) have been developed with the objective of improving the mechanical properties and biocompatibility of metallic biomaterials. Since CP titanium has poor mechanical properties such as low shear strength, it is not desirable for dental and orthopedic implants. Moreover, Ti-6Al-4V ELI alloy is not feasible for such implants because of the cytotoxicity of vanadium (V). Most of the recently developed alloys are β-type titanium alloys that have a considerably lower Young's modulus as compared to that of α- or (α + β)-type titanium alloys. Another advantage of these alloys is that it is relatively easy to control their mechanical properties by thermomechanical treatment.

The biocompatible Ti-29Nb-13Ta-4.6Zr alloy (TNTZ) developed by the authors has a high potential for usage in biomedical applications because of its superior mechanical properties such as high specific strength and elongation.[1–5] As-solutionized TNTZ has a low Young's modulus of around 60 GPa, very low cytotoxicity similar to that of CP titanium, and good biocompatibility with living tissues.[6] However, its biocompatibility is inadequate and it lacks bioactivity—the ability to form a chemical bonding directly with bones. The stems of artificial joints, dental implants, etc., made of metallic materials are required to bond strongly with living bones. However, the stems cannot form a chemical bond with living bones by themselves.

Bioactive ceramic surface modification is effective for improving the biocompatibility of TNTZ. Calcium phosphate ceramics such as hydroxyapatite ($Ca_{10}(PO_4)_6OH_2$; HAP), β-calcium pyrophosphate (β-$Ca_2P_2O_7$; CPP), and β-tricalcium phosphate (β-$Ca_3(PO_4)_2$; β-TCP) exihibit bioactivity.[7,8] Bioactivity is required in some regions of artificial substitutes for hard tissues. Many types of HAP and TCP coating methods on titanium or titanium alloys have been reported so far.[9–16] Among these methods, alkali solution treatments are simple and highly suitable for TNTZ.[17,18] In this study, the formability and morphology of the alkali-solution-treated surface of TNTZ were investigated before and after immersion in a simulated body fluid (SBF).

2. Experimental Procedures

2.1 Material

The materials used in this study are hot forged bars of TNTZ (Nb: 29.0, Ta: 12.7, Zr: 4.4, Fe: 0.04, O: 0.01, C: 0.01,

*Graduate Student of Toyohashi University of Technology, Toyohashi 441-8580, Japan

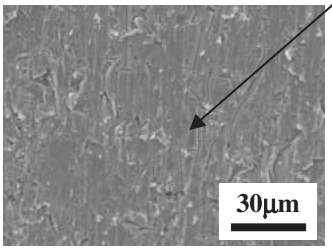

Element	Mass%
Na	3.06
O	34.4
Ti	31.3
Nb	18.8
Ta	8.48
Zr	4.05

(a) 3 mol / 86.4 ks

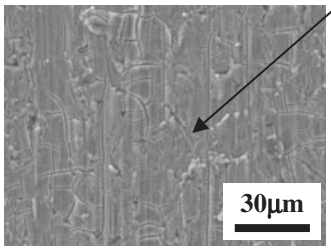

Element	Mass%
Na	6.62
O	37.1
Ti	29.2
Nb	16.9
Ta	6.45
Zr	3.67

(b) 3 mol / 172.8 ks

Fig. 1 SEM micrographs and results of EDS on specimen surfaces of TNTZ after dipping in 3 kmol·m^{-3}-NaOH solutions at 333 K for (a) 86.4 ks and (b) 172.8 ks.

N: 0.07, Ti: bal. mass%) with a diameter of 11 mm. The TNTZ bars were solution treated in vacuum at 1063 K, which is greater than the β-transus temperature of TNTZ (around 1013 K), for 3.6 ks. The as-solutionized TNTZ formed is referred to as $TNTZ_{ST}$.

2.2 Alkali treatment

The $TNTZ_{ST}$ bars with a diameter and thickness of 10 and 2.0 mm, respectively, were polished with a wet emery paper with a grid of # 600; then, they were washed with pure acetone and distilled water in an ultrasonic cleaner. Further, they were subjected to alkali treatment by immersing in NaOH aqueous solutions with concentrations of 3, 5, and 10 kmol·m^{-3} at 333 K for 86.4 and 172.8 ks. After the alkali treatment, the specimens were washed with distilled water and dried at 313 K for 86.4 ks. The alkali-treated specimens are referred to as $TNTZ_{AT}$.

2.3 Baking treatment

$TNTZ_{AT}$, which was subjected to an optimum alkali treatment to form HAP, was subjected to baking treatment at 673, 773, 873, and 973 K for 3.6 ks, where the temperature rising rate was 8.3×10^{-2} K/s; this was followed by furnace cooling in order to densify the compound on its surface and investigate the change in the formability of HAP.

2.4 SBF treatment

In order to investigate the formation of HAP on the $TNTZ_{AT}$ surfaces, the specimens were soaked in the SBF (Na^+: 142, K^+: 5, Mg^+: 1.5, Ca^+: 2.5, Cl^-: 103, HCO_3^-: 27, HPO_4^{2-}: 1, SO_4^{2-}: 0.5 mol/m^3) having pH and ion concentrations similar to human blood plasma (Na^+: 142, K^+: 5, Mg^+: 1.5, Ca^+: 2.5, Cl^-: 103.8, HCO_3^-: 4.2, HPO_4^{2-}: 1, SO_4^{2-}: 0.5 mol/m^3) at 310 K for 604.8 ks to 1209.6 ks. The SBF was replaced every 259.2 ks. Here, the pH and temperature of the SBF was buffered at 7.4 with tris-hydroxymethyl aminomethane ($(CH_2OH)_3CNH_3$) and hydrochloric acid (HCl) at 310 K.

2.5 Evaluation of microstructure

Microstructural evaluations were carried out using a scanning electron microscopy (SEM) at 20 kV in combination with an energy dispersion spectroscopy (EDS), an Auger electron spectrometry (AES) at 10 kV, a thin film X-ray diffractometer (XRD) using a Cu-K_α line with an accelerating voltage of 40 kV and a tube current of 250 mA, and an X-ray photoelectron spectroscopy (XPS) using a Al-K_α line at 10 kV.

2.6 Mechanical test

Columnar specimens of $TNTZ_{AT}$ with diameter and height of 10 and 20 mm, respectively, were used to evaluate the tensile bonding strength of the coating layers. A bonding agent for dental applications (orthomite super bond) was applied to the surface of the coating layer of each specimen. The surface coated with the bonding agent was then bonded with a columnar stainless steel fixture whose size was identical to that of the columnar specimens. Subsequently, the bonded specimens were dried in air at room temperature for 86.4 ks and subjected to the tensile bonding test.[19] The tests were conducted at a crosshead speed of 1.67×10^{-5} m/s in air at room temperature using an Instron-type tensile testing machine.

3. Results and Discussion

3.1 Morphologies on specimen surface of $TNTZ_{ST}$ subjected to various alkali treatments

Figures 1, 2 and 3 show the SEM micrographs and the results of EDS for the alkali treated $TNTZ_{ST}$ ($TNTZ_{AT}$) specimen surfaces in 3, 5, and 10 kmol·m^{-3} NaOH solutions at 333 K for 86.4 and 172.8 ks. Several compounds with micro-cracks composed of Na, O, and alloying elements of TNTZ can be observed on the specimen surface of $TNTZ_{AT}$ in 3 kmol·m^{-3} NaOH solution, as shown in Fig. 1. The compounds appear to be some type of Na-O-X (X is Ti, Nb, Ta, and Zr). As the immersion time is increased from 86.4 ks to 172.8 ks, the amounts of Na and O increase. In particular, the amount of Na in the solution for 172.8 ks is around twice that for 86.4 ks. However, the alloying elements exhibit a reverse trend. The cracks in the Na-O-X compound of $TNTZ_{AT}$ in 5 kmol·m^{-3} NaOH solutions grow partially when compared with those in 3 kmol·m^{-3} NaOH solutions, as shown in Fig. 2. The change in the amounts of Na and O for $TNTZ_{AT}$ in 5 kmol·m^{-3} NaOH solutions from 86.2 ks to 172.8 ks is almost similar to that for 3 kmol·m^{-3} NaOH solutions, although there is an overall increase in their amounts. Many very coarse cracks in the Na-O-X compounds appear on the specimen surface of $TNTZ_{AT}$ in 10 kmol·m^{-3} NaOH solutions for 86.4 and 172.8 ks, as shown in Fig. 3. The surface of crack mainly seems to be composed of oxide (mainly TiO_2) and a small amount of Na-O-X compounds

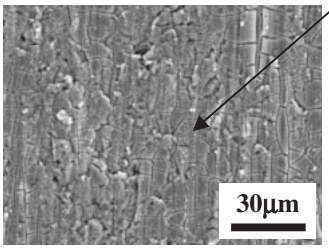

Element	Mass%
Na	5.01
O	32.8
Ti	33.8
Nb	16.4
Ta	8.70
Zr	3.27

(a) 5 mol / 86.4 ks

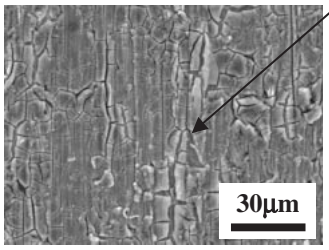

Element	Mass%
Na	8.44
O	37.4
Ti	25.9
Nb	17.3
Ta	7.81
Zr	3.15

(b) 5 mol / 172.8 ks

Fig. 2 SEM micrographs and results of EDS on specimen surfaces of TNTZ after dipping in 5 kmol·m^{-3}-NaOH solutions at 333 K for (a) 86.4 ks and (b) 172.8 ks.

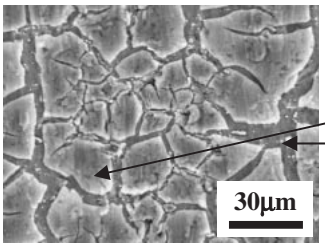

Element	Mass%
Na	6.18
O	38.5
Ti	27.5
Nb	16.6
Ta	8.46
Zr	2.73

Element	Mass%
Na	1.02
O	34.3
Ti	34.1
Nb	18.1
Ta	7.95
Zr	4.31

(a) 10 mol / 86.4 ks

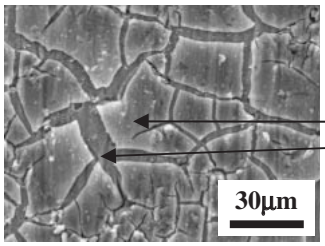

Element	Mass%
Na	8.61
O	39.0
Ti	26.8
Nb	16.4
Ta	6.68
Zr	2.63

Element	Mass%
Na	1.29
O	33.8
Ti	32.1
Nb	19.7
Ta	9.37
Zr	3.74

(b) 10 mol / 172.8 ks

Fig. 3 SEM micrographs and results of EDS on specimen surfaces of TNTZ after dipping in 10 kmol·m^{-3}-NaOH solutions at 333 K for (a) 86.4 ks and (b) 172.8 ks.

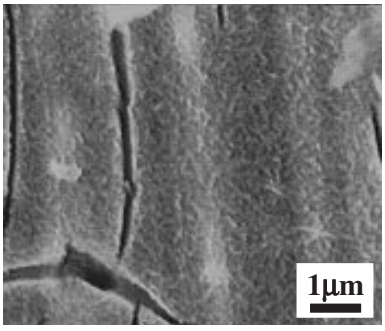

Fig. 4 Representative SEM micrograph on specimen surface of TNTZ after dipping in 5 kmol·m^{-3}-NaOH solutions at 333 K for 172.8 ks with a high magnification.

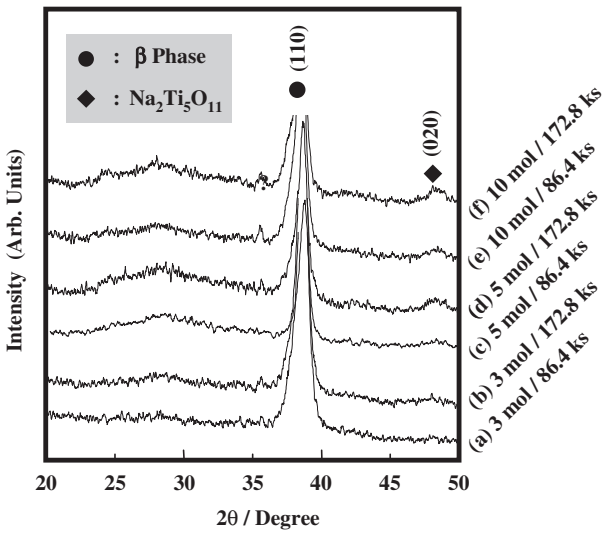

Fig. 5 XRD profiles of specimen surfaces of TNTZ$_{AT}$ in 3, 5 and 10 kmol·m^{-3}-NaOH solutions for 86.4 and 172.8 ks.

because the amount of Na on the coarse crack is around 1 mass%.

Using high magnification, a very fine reticulate structure can be observed on the Na-O-X compound for all the specimen surfaces of TNTZ$_{AT}$, as representatively shown in Fig. 4. However, this structure was not observed on the very coarse cracks.

Figure 5 shows the XRD profiles of the specimen surface of TNTZ$_{AT}$ in 3, 5, and 10 kmol·m^{-3} NaOH solutions for 86.4 and 172.8 ks. The XRD profile reveals that a β-phase$_{(110)}$ exists on the specimen surface of TNTZ$_{AT}$ in 3 kmol·m^{-3} NaOH solutions for 86.4 ks. However, a broad diffraction peak ranging from 23 to 35 degrees appears on the specimen surface of TNTZ$_{AT}$ in 3 kmol·m^{-3} NaOH solutions for 172.4

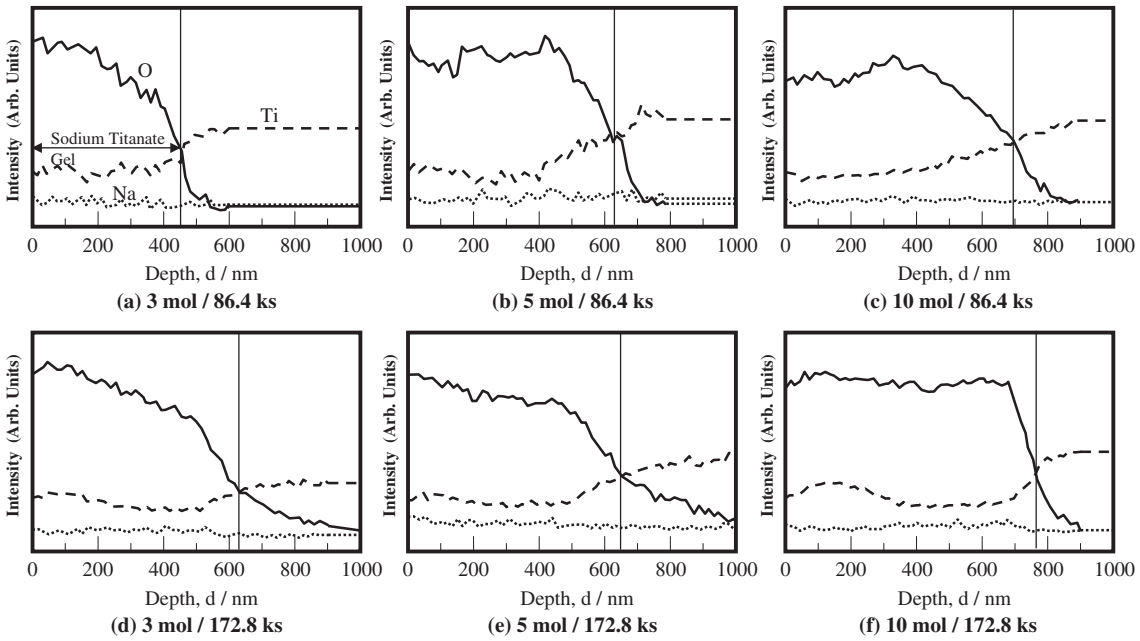

Fig. 6 Results of AES on specimen surfaces of $TNTZ_{AT}$ in 3, 5 and 10 kmol·m^{-3}-NaOH solutions at 333 K for 86.4 ks and 172.8 ks.

ks as well. The broad diffraction peak seems to correspond to that of amorphous sodium titanate ($Na_2Ti_5O_{11}$ or $NaTi_6O_{12}$); it was difficult to distinguish between them on the basis of their diffraction angles because the values of their diffraction angles were very close to each other. It is considered that the thickness of sodium titanate film of $TNTZ_{AT}$ in 3 kmol·m^{-3} NaOH solutions for 86.4 ks is much lesser than that of $TNTZ_{AT}$ in these solutions for 172.8 ks, although their morphologies on the specimen surface were very similar; this is shown in Fig. 1.

The XRD profiles show a diffraction peak of sodium $titanate_{(020)}$ ($Na_2Ti_5O_{11}$) on the specimen surfaces of $TNTZ_{AT}$ immersed in 5 and 10 kmol·m^{-3} NaOH solutions for 86.4 and 172.8 ks at a diffraction angle of around 48 degrees. As the immersion time is increased, the diffraction peak is also increases.

It is well known that CP titanium and its alloys are covered with a titanium oxide film such as TiO_2. The oxide film on TNTZ might be composed of many types of oxide such as Nb_2O_5, Ta_2O_5, and ZrO_2 as well as TiO_2. The atomic ratio of Ti, Nb, Ta, and Zr in the oxides film on $TNTZ_{ST}$ was estimated to be around 80%, 12%, 3% and 5%, respectively, by XPS. The oxide film is mainly composed of TiO_2 and Nb_2O_5. The predominantly dissolution reaction of the titanium oxide film in the alkali solution is as follows:[13)]

$$TiO_2 + OH^- \rightarrow HTiO_3^- \quad (1)$$

A small niobium oxide film may dissolve according to the following reaction:[20)]

$$Nb_2O_5 + 2OH^- \rightarrow 2NbO_3^- + H_2O \quad (2)$$

Hence, the negatively charged specimen surfaces are combined with positively charged alkali ions resulting in the formation of a sodium titanate hydrogel. When immersed into the SBF, the Na^+ ion is released from the hydrogel layer and then the positively charged hydronium (H_3O^+) ion in the SBF is incorporated with the Ti-OH group on the specimen surface.

Figure 6 shows the AES results for $TNTZ_{AT}$ immersed in 3, 5, and 10 kmol·m^{-3} NaOH solutions at 333 K for 86.4 and 172.8 ks as a function of the distance from the specimen surface. The thickness of the oxide film on TNTZ was measured to be around 10 nm before the alkali treatment, when the intersecting points between the oxygen and titanium intensity profiles obtained from AES were set at an interface between the oxide film and matrix.[17)] After the alkali treatment, a sodium titanate and niobate film composed of titanium, oxygen, and sodium is observed. The thickness of the reticulate product appears to increase proportionally from 400 nm to 800 nm with an increase in the molar concentration of NaOH solution and the immersion time in the solution.

3.2 Formability of HAP on specimen surface of $TNTZ_{AT}$

Table 1 shows the formability of HAP on the specimen surface of $TNTZ_{AT}$ immersed in the SBF for 604.8 and 1209.6 ks after immersing in 3, 5, and 10 kmol·m^{-3} NaOH solutions at 333 K for 86.4 and 172.8 ks. HAP is not formed on all the specimen surfaces of $TNTZ_{AT}$ immersed in the SBF for 604.8 ks. HAP is formed only on the specimen surfaces of $TNTZ_{AT}$ immersed in the SBF for 1209.6 ks after immersing in 3, 5, and 10 kmol·m^{-3} NaOH solutions. The HAP formation on the specimen surfaces of $TNTZ_{AT}$ immersed in 3 and 5 kmol·m^{-3} NaOH solutions is partial and complete, respectively. On the other hand, HAP is partly exfoliated from the specimen surface of $TNTZ_{AT}$ immersed in the 10 kmol·m^{-3} NaOH solutions, as shown in Fig. 7.

The bonding strength between $TNTZ_{AT}$, where the alkali treatment was carried out in 5 kmol·m^{-3} NaOH solutions for 172.8 ks, and HAP layer was around 2 MPa, which was half or less than half the value required for biomedical applications.[18)] The HAP layer on the specimen surface of $TNTZ_{AT}$

Table 1 Formability of HAP on specimen surface of $TNTZ_{AT}$ in 3, 5 and 10 kmol·m^{-3}-NaOH solutions at 333 K for 86.4 ks and 172.8 ks followed by immersion in SBF for 604.8 ks and 1209.6 ks.

Conditions of NaOH Treatments	Immersion Time	
	604.8 ks	1209.6 ks
3 mol/86.4 ks	×	×
5 mol/86.4 ks	×	×
10 mol/86.4 ks	×	×
3 mol/172.8 ks	×	△
5 mol/172.8 ks	×	○
10 mol/172.8 ks	×	○*

○: Specimen surface was completely covered with HAP.
△: Specimen surface was partly covered with HAP.
×: HAP was not formed on specimen surface.
*: HAP was partly exfoliated.

was completely removed. The chemical composition of the fracture surface of $TNTZ_{AT}$ was almost similar to that of the matrix. The amounts of Ca, P, and Na were negligibly low or less than 0.1 mass%. It seems that it is required to raise the bonding strength by a densification of the sodium titanate and niobate film by carrying out a baking treatment after the alkali treatment.[21)]

The exchange of the Na ion with the hydronium ion in the SBF results in an increase in the pH of the surrounding fluid near the specimen surface. This increase leads to an increase in the ionic activity product of HAP according to the following equilibrium in the SBF:

$$10Ca^{2+} + 6PO_4^{3-} + 2OH^- \leftrightarrow Ca_{10}(PO_4)_6(OH)^2 \quad (3)$$

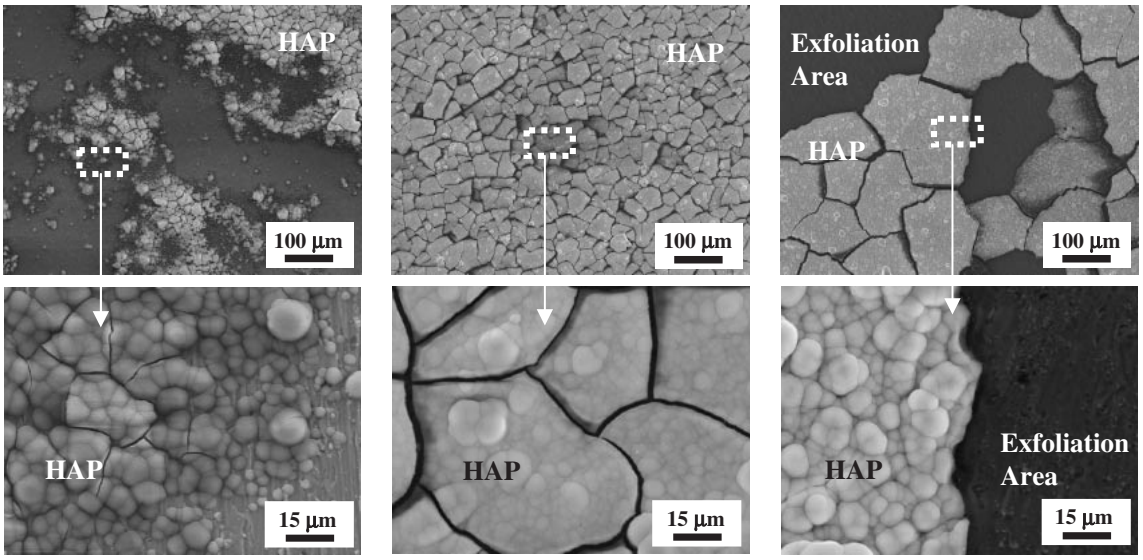

Fig. 7 SEM micrographs of specimen surfaces of $TNTZ_{AT}$ in 3, 5 and 10 kmol·m^{-3}-NaOH solutions followed by immersion in SBF for 1209.6 ks.

Table 2 Formability of HAP on specimen surfaces of CP Ti, CP Nb, CP Ta and CP Zr as functions of alkali treatment conditions and immersion time in SBF.[22–25)]

Metal	NaOH Treatment			Baking Treatment	SBF Treatment					
	Concentration (Mol)	Temperature (K)	Immersion Time (ks)	Temperature (K)	Immersion Time (ks)					
					43.2	86.4	259.2	604.8	1209.6	2419.2
CP-Ti	5	333	86.4	873	×	○	○	○	○	○
CP-Nb	0.5	333	86.4	—	—	—	—	—	×	—
	1				—	—	—	—	×	—
	2				—	—	—	—	×	—
CP-Ta	0.2	333	86.4	—	—	—	—	○	○	○
	0.5				—	—	—	○	○	○
	5				—	—	—	×	×	×
	0.5		259.2	573	—	—	○	○	○	○
CP-Zr	1	368	86.4	—	—	—	—	×	×	×
	5				—	—	—	○	○	○
	15				—	—	—	○	○	○

○: Specimen surface was covered with HAP.
×: HAP was not formed on specimen surface.

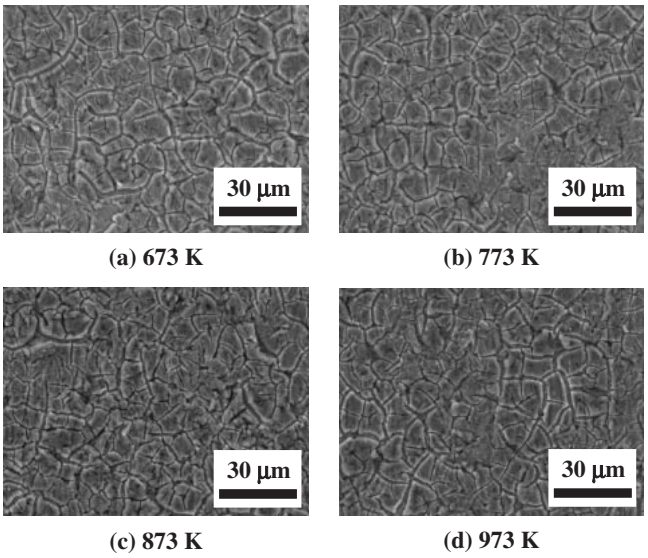

Fig. 8 SEM micrographs of specimen surfaces of $TNTZ_{AT}$ in 5 kmol·m^{-3}-NaOH solutions for 172.8 ks followed by baking treatments at 673, 773, 873 and 973 K for 3.6 ks.

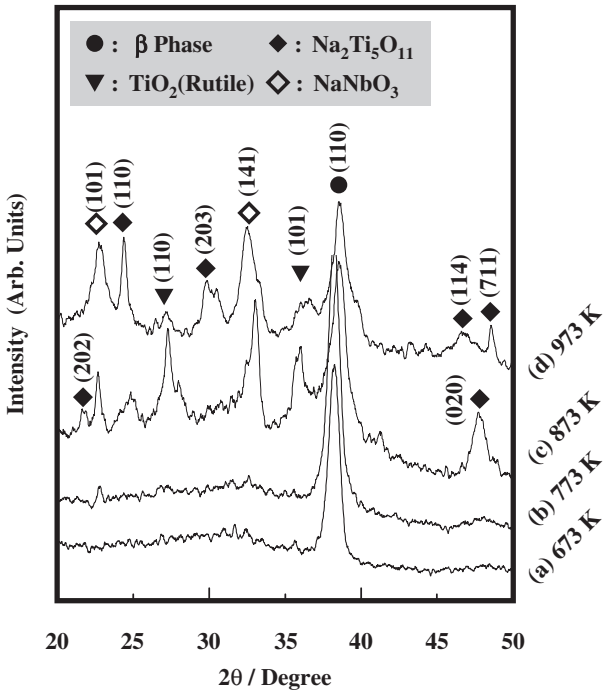

Fig. 9 XRD profiles of specimen surfaces of $TNTZ_{AT}$ in 5 kmol·m^{-3}-NaOH solutions for 172.8 ks followed by baking treatments at 673, 773, 873 K for 3.6 ks.

The apatite nuclei grow with increase in the consumption of the calcium and phosphate ions from the surrounding fluid. It has been reported that HAP formation on the specimen surface of CP titanium is enhanced by increasing the molar concentration and the immersion time of the alkali solution.[22] In particular, the HAP formation is complete on the specimen surface immersed in the SBF for 172.8 ks after immersing in 5 to 10 kmol·m^{-3} NaOH solution at temperatures between 313 and 333 K for 86.4 ks. A similar trend is observed for $TNTZ_{AT}$, although the HAP formation takes much longer time compared to the case of alkali-treated CP titanium. The HAP formation might be delayed due to the existence of different types of oxide films according to the alloying elements. Table 2[23–26] shows the formability of HAP on the specimen surface for CP titanium, CP niobium, CP tantalum, and CP zirconium immersed in the SBF for several immersion times after carrying out certain alkali treatments. The formation of HAP on the specimen surface of CP titanium is the fastest of all the elements. CP tantalum and CP zirconium have a relatively high formability of HAP. On the other hand, CP niobium seems to have a lower formability of HAP as compared to the others, although the data reported has been very poor. Therefore, a further detailed investigation is required to clarify this issue.

3.3 Effect of baking treatment on the formability of HAP

Figure 8 shows the SEM micrographs of $TNTZ_{AT}$ in 5 kmol·m^{-3} NaOH solutions at 333 K for 172.8 ks followed by baking treatments at 673, 773, 873, and 973 K for 3.6 ks. The higher the baking temperature, the clearer the crack is as compared to that on the specimen surface of $TNTZ_{AT}$ in 5 kmol·m^{-3} NaOH solutions at 333 K for 172.8 ks without the baking treatment. This is the reason why the moisture content in the amorphous sodium titanate and niobate film evaporated, consequently shrinking the film. Figure 9 shows the XRD profiles of the specimen surface of $TNTZ_{AT}$ in 5 kmol·m^{-3} NaOH solutions for 172.8 ks, followed by baking treatments at 673, 773, 873, and 973 K for 3.6 ks. The XRD profiles of $TNTZ_{AT}$ subjected to baking treatment at 673 and 773 K reveal a broad diffraction peak ranging from 23 to 35 degrees and diffraction peaks of β-phase. An amorphous sodium titanate and niobate film is present on the specimen surface as well as on $TNTZ_{AT}$ without baking treatment. On the other hand, the XRD profiles of $TNTZ_{AT}$ subjected to baking treatments at 873 and 973 K consist of the diffraction peaks of β-phase, TiO_2, sodium titanate, and sodium niobate. Growth of the oxide film and crystallization of amorphous sodium titanate and niobate film occurs at these temperatures.

Figures 10 and 11 show the SEM micrographs and the XRD profiles of the specimen surfaces of $TNTZ_{AT}$ in 5 kmol·m^{-3} NaOH solutions at 333 K for 172.8 ks subjected to baking treatments at 673, 773, 873, and 973 K, followed by immersion in the SBF for 1209.6 ks. Some spherical particles with diameters ranging from 2.0 to 5.0 μm are formed on all the specimen surfaces, which are identified as HAP by an XRD analysis, as shown in Fig. 11. As the baking temperature is increased, the volume fraction of the particle decreases in the order of approximately 81, 67, 45 and 37%. In other words, the higher the baking temperature, the worse the formability of HAP. Diffraction peaks of crystalline sodium titanate and niobate and TiO_2 exist at baking temperatures of 873 and 973 K, as shown in Fig. 11. This trend is almost similar to that of CP titanium, although the immersion time of CP titanium in the SBF up to the formation of HAP is much lesser than that of $TNTZ_{AT}$, as shown in Table 3.[22] The HAP layer is formed on the specimen surface of CP titanium subjected to a baking treatment at 673 K for 86.4 ks, when an optimum alkali solution treatment is carried out. The formation rate of CP

titanium is over seven times greater than that of $TNTZ_{AT}$. The reason for the delay in the case of $TNTZ_{AT}$ is that the release rate of Na^+ ion from the crystalline sodium titanate film decreases in the SBF as compared to the amorphous film. Thus, it is difficult to form the Ti-OH groups (a hydrate titania film) on the surface, which are exchanged between the Na^+ and H_3O^+ ions in the SBF.[22)]

From the results obtained, it is required to increase the immersion time in the SBF to over 1209.6 ks in order to obtain fully covered and densified HAP on the specimen surface of $TNTZ_{AT}$ in 5 kmol·m^{-3} NaOH solutions. The formability of HAP on the surface of TNTZ is relatively lower than not only α-type titanium (*e.g.*, CP-titanium) but also an ($\alpha + \beta$)-type titanium alloy (*e.g.*, Ti-6Al-4V ELI), and β-type titanium alloy (*e.g.*, Ti-15Mo-5Zr-3Al) by alkali solution treatment.[23)] The reason for the delay in the formation of HAP is considered to be to existence of the sodium niobate film, which seems to delay the exchange between the Na^+ and H_3O^+ ions, in addition to the baking treatment. However, further investigation is required to confirm it.

4. Conclusions

The formability of the specimen surface of a β-type titanium alloy—Ti-29Nb-13Ta-4.6Zr (TNTZ)—was investigated for biomedical applications subjected to alkali solution treatment before and after immersing in a simulated body fluid (SBF). The following results were obtained.

(1) A reticulate structure with several large cracks and mainly composed of sodium titanate and niobate films with a thickness of 400 nm to 800 nm is formed on the specimen surface of TNTZ after immersion in 3, 5, and 10 kmol·m^{-3} NaOH solutions for 86.4 and 172.8 ks. As the concentration of the alkali solution and the immersion time is increased, the formability of HAP is improved because of the increase of the amount of oxygen and sodium in the sodium titanate and niobate film.

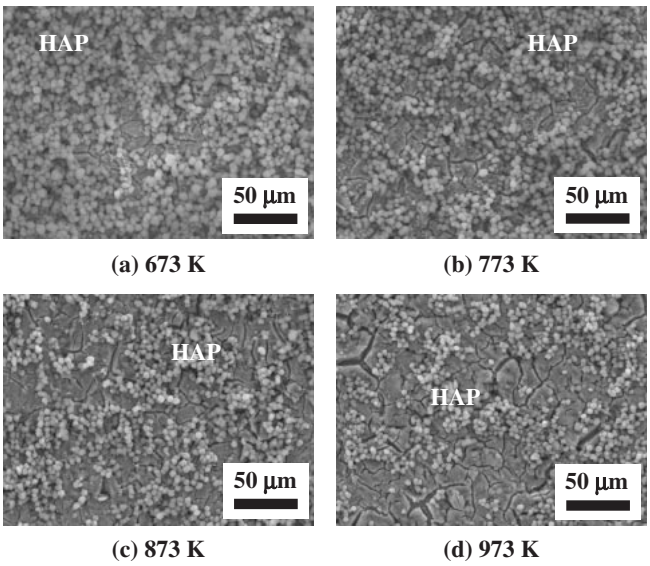

Fig. 10 SEM micrographs of specimen surfaces of $TNTZ_{AT}$ in 5 kmol·m^{-3}-NaOH solutions for 172.8 ks followed by immersion in SBF for 1209.6 ks after baking treatments at 673, 773, 873 and 973 K for 3.6 ks.

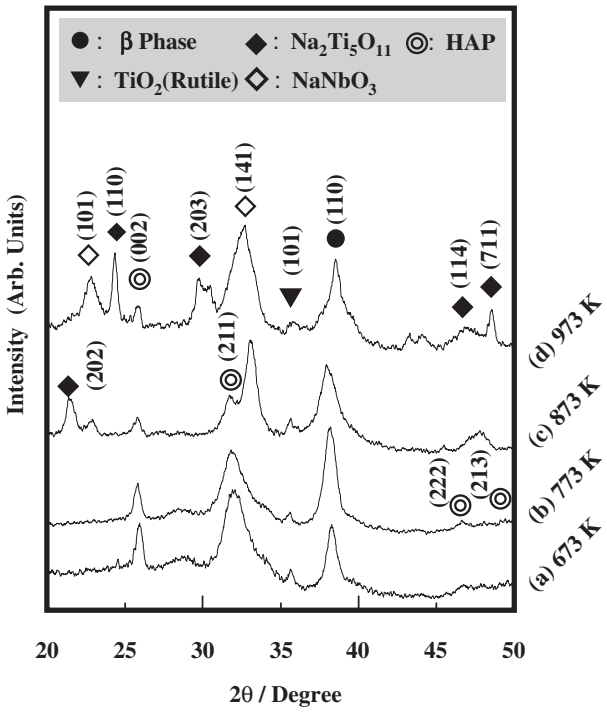

Fig. 11 XRD profiles of specimen surfaces of $TNTZ_{AT}$ in 5 kmol·m^{-3}-NaOH solutions followed by immersion in SBF for 1209.6 ks after baking treatments at 673, 773, 873 and 973 K for 3.6 ks.

Table 3 Formability of HAP on specimen surfaces of CP Ti as functions of baking temperature and immersion time in SBF.[21)]

NaOH Treatment			Baking Treatment	SBF Treatment					
Concentration (Mol)	Temperature (K)	Immersion Time (ks)	Temperature (K)	Immersion Time (ks)					
				43.2	86.4	259.2	604.8	1209.6	2419.2
5	333	86.4	0	×	○	○	○	○	○
			673	×	×	○	○	○	○
			773	×	×	○	○	○	○
			823	×	×	○	○	○	○
			873	×	×	○	○	○	○
			973	×	×	×	○	○	○
			1073	×	×	×	○	○	○

○: Specimen surface was covered with HAP.
×: HAP was not formed on specimen surface.

(2) HAP is partly and completely formed on the specimen surfaces of alkali-treated TNTZ in 3 and 5 kmol·m^{-3} NaOH solutions for 1209.6 ks, respectively. On the other hand, exfoliation of HAP is observed on the specimen surface of alkali-treated TNTZ in the 10 kmol·m^{-3} NaOH solution for 1209.6 ks. The alkali treatment at 333 K in 5 kmol·m^{-3} NaOH solutions for 172.8 ks is proposed to be an excellent condition to quickly form HAP and fully cover the surface of TNTZ with it.

(3) The bonding strength between TNTZ, subjected to alkali treatment at 333 K in 5 kmol·m^{-3} NaOH solutions for 172.8 ks, and HAP is around 2 MPa, which is half or less than half the value required for biomedical applications.

(4) The addition of a baking treatment after the alkali treatment in order to improve the bonding strength degrades the HAP formability. Furthermore, the formability decreases with an increase in the baking temperature.

Acknowledgements

Some parts of this study are supported by The Light Metal Education Foundation (Osaka, Japan). One of the author (TA) would like to express great thanks to Assistant Professor H. Kimura and Technical officer N. Ohtsu, IMR, Tohoku University (Sendai, Japan) for microstructural evaluations by an AES and XPS.

REFERENCES

1) D. Kuroda, M. Niinomi, M. Morinaga, Y. Kato and T. Yashiro: Mater. Sci. Eng. A **A243** (1998) 244–249.
2) M. Niinomi, D. Kuroda, K. Fukunaga, M. Morinaga, Y. Kato, T. Yashiro and A. Suzuki: Mater. Sci. Eng. A **A263** (1999) 193–199.
3) M. Niinomi: Metal. Mater. Trans. A **32A** (2001) 477–486.
4) M. Niinomi: Biomaterials **24** (2003) 2673–2683.
5) M. Niinomi, T. Hattori and S. Niwa: *Biomaterials in Orthopedics*, Eds. M. J. Yaszemski, D. J. Trantolo, K. U. Lewandrowski, V. Hasirci, D. E. Altobelli and D. L. Wise, (Marcel Dekker, INC, 2004) pp. 41–62.
6) M. Niinomi, T. Hattori, K. Morikawa, T. Kasuga, A. Suzuki, H. Fukui and S. Niwa: Mater. Trans. **43** (2002) 2970–2977.
7) L. L. Hench: Bioceramics **74** (1991) 1487–1510.
8) R. H. Doremus: Bioceramics **27** (1992) 285–297.
9) W. R. Lancefield: *An Introduction to Bioceramics*, Edts. L. L. Hench and J. Wilson, (1993) pp. 223–238.
10) Y. Fan, K. Duan and R. Wang: Biomater. **26** (2005) 1623–1632.
11) T. Nonami, K. Naganuma and T. Kameyama: Materia Japan **37** (1998) 856–858.
12) S. Ding, T. Huang and C. Kao: Surf. Coating Tech. **165** (2003) 248–257.
13) H. M. Kim, F. Miyaji, T. Kokubo and T. Nakamura: J. Cera. Soc. JPN **105** (1997) 111–116.
14) T. Hanawa, M. Kon, H. Ukai, K. Murakami, Y. Miyamoto and K. Asaoka: J. Biomed. Mater. Res. **34** (1997) 273–278.
15) V. Nelea, C. Morosanu, M. Iliescu and I. N. Mihailescu: Surf. Coating Tech. **173** (2003) 315–322.
16) F. Liang, L. Zhou and K. Wang: Surf. Coating Tech. **165** (2003) 133–139.
17) B. H. Lee, Y. D. Kim, J. H. Shin and K. H. Lee: J. Biomed. Mater. Res. **61** (2002) 466–473.
18) T. Nonami, C. Takahashi and S. Tsutsumi: J. Japanese Soc. Biomater. **13** (1995) 261–265.
19) T. Akahori, M. Niinomi, Y. Koyanaga, T. Kasuga, H. Toda, H. Fukui and M. Ogawa: Materials Transactions **46** (2005) 1564–1569.
20) R. Rosenberg, D. Starosvetsky and I. Gotman: J. Mater. Sci. Letters **22** (2003) 29–32.
21) T. Miyazaki, H. M. Kim and T. Kokubo: J. Mater. Sci. (Mater. Medicine) **13** (2002) 651–655.
22) H. M. Kim, F. Miyaji, T. Kokubo and T. Nakamura: J. Mater. Sci. (Mater. Medicine) **8** (1997) 341–347.
23) H. M. Kim, F. Miyaji, T. Kokubo and T. Nakmure: J. Biomed. Mater. Res. **32** (1996) 409–417.
24) T. Miyazaki, H. Kim, T. Kokubo, C. OHtsuki and T. Nakamura: J. Cera. Soc. Japan **109** (2001) 923–933.
25) T. Miyazaki, H. M. Kim, F. Miyaji, T. Kokubo and H. Kato: J. Biomed. Mater. Res. **50** (2000) 35–42.
26) M. Uchida, H. M. Kim, F. Miyaji, T. Kokubo and T. Nakamura: Biomater. **23** (2002) 313–317.